NOVEL TRANSPORT PROPERTIES OF NANOSTRUCTURED α-Fe$_2$O$_3$

P. Brahma[1ξ], S. Dutta[2]

[1] Department of Physics, Gurudas College, Kolkata – 700054, India
[2] Department of Physics, Rammohan College, Kolkata -700009, India

Keywords: Mechanical milling, Ferric oxide, Nanostructure, Transport properties

Abstract

Nanophase materials with an average grain sizes ranging from 2 to 20 nm exhibit novel properties relative to conventional materials. Recently, we reported that the mechanical milling of Fe$_3$O$_4$ powders produced nanometer sized particles (~7 nm) which exhibited a phase transition from cubic (Fe$_3$O$_4$) to hexagonal (α-Fe$_2$O$_3$) phase. In this paper, we present results on the synthesis of nanosized α-Fe$_2$O$_3$ produced by mechanical milling for 1 to 10 h. Some unusual electrical conductivity characteristics were observed. The X-ray diffraction analyses show only the presence characteristic lines of hematite in the ball milled samples. Particle sizes measured from X-ray line broadening varied from 7 to 11 nm. TEM micrograph for the ball milled samples show distribution of particle size. A drastic change of electrical resistivity has been observed from the electrical measurements of different ball milled samples. The resistivity variation of the unmilled sample can be ascribed to typical band conduction. A decrease of about two orders of magnitude of resistivity was observed for the specimen ball milled for 10 h. The resistivity variation of the two activated processes was observed with activation energies of ~ 0.06 and ~ 0.7eV, respectively. Large and small particle sizes are responsible for the two activation energies.

Introduction

Nanophase materials with an average grain sizes ranging from 5 to 20 nm, exhibit properties that are often different and novel vis-à-vis conventional materials [1]. The electronic, magnetic, optical and chemical properties of the materials have been found to vary differently from those of the bulk form and depend sensitively on size, shape and composition [2]. A number of techniques have been developed to synthesize nanoparticles. Inert gas condensation [3], laser ablation [4], supersonic expansion method [5], sputtering technique [6] are few among the physical methods. Various chemical methods such as sol-gel technique [7], reduction of melt quenched glasses [8], (AOT)/heptane inverse micell method [9], and electrodeposition method have also been employed [10].

However, material processing by these methods has the following shortcomings. In some cases methods are not cost effective and yield of materials is very small in some cases. Mechanical alloying is a powerful method for the production of a variety of fine particles [11]. Apart from quantum size effects and surface and interface effects, a decrease in the particle size causes definite and systematic changes in the crystal symmetry and lattice parameters, particularly in oxide nanoparticles [12,13]. In the present work we report on the synthesis of nanometer sized α-Fe$_2$O$_3$ by mechanical milling in normal atmosphere. Some unusual electrical conductivity characteristics were observed. The results are reported in this paper.

Experimental

α-Fe$_2$O$_3$ (99%) procured from Aldrich was employed for milling in Fritsch Pulverisette 5 planetary ball mill. Hardened steel vials of 8×10^{-5} m^3 volume and hardened steel vials of 0.01 m diameter were used for milling. Hematite powder (α-Fe$_2$O$_3$) was crushed and disintegrated in the grinding bowl, keeping the ball to powder mass ratio 20:1. The rotational speed of the mill was set at 300 rpm. The powder was milled in normal atmosphere without any additive under 'closed' milling condition. Small quantities of sample were taken from the bowl after 1,2,4,6 and 10 hrs of milling in order to check the phase formation during milling time by X-Ray diffraction technique. The X-Ray diffraction Patterns of the samples were recorded using Ni-filtered Cu-K$_\alpha$ radiation from a highly stabilized Philips X-Ray generator (PW 1130) operating at 40 kV and 25 mA, coupled with a Philips X-Ray diffractometer consisting of a PW 1710 controller, PM 8203A recorder and PW 1080/81 goniometer. The step scan data (of step size 0.02^o 2θ and counting time 15-20 s depending on the peak intensity) for the entire angular range of the experimental samples were recorded in a Philips PC, coupled with the diffractometer. The instrumental standard used is a specially prepared Si sample [14]. The transmission electron microscopy (JEOL 2010) was carried out for the samples milled for 1h and 10 h.

For electrical measurements, discs of about 0.01 m diameter and 2×10^{-3} m thickness were prepared by cold pressing the ball milled powder employing a 5 ton load. Silver paint electrodes were applied on the two opposite faces of the samples using paste supplied by M/S Acheson Colloiden BV, Netherlands. DC electrical resistances were measured by a 617 Kiethley Electrometer over the temperature range 195-300 K under a vacuum of ~ 10^{-2} Torr. Ohmic contact was checked by confirming the linearity of the V-I characteristics.

Results and Discussion

Figure1 shows the X-ray diffraction patterns of α- Fe$_2$O$_3$ powder samples in both unmilled and milled states. The X-ray diffraction patterns show only the hematite characteristic lines. No contamination from the grinding medium was detected. A broadening of these lines for the milled samples can be noticed with respect to bulk samples. To estimate the average size of the

---

[ξ] email: pradip_brh@yahoo.com

particles, lattice parameter and root mean square (RMS) strain, Rietveld profile [15] analyses were performed. The extracted parameters are summarized in Table 1.
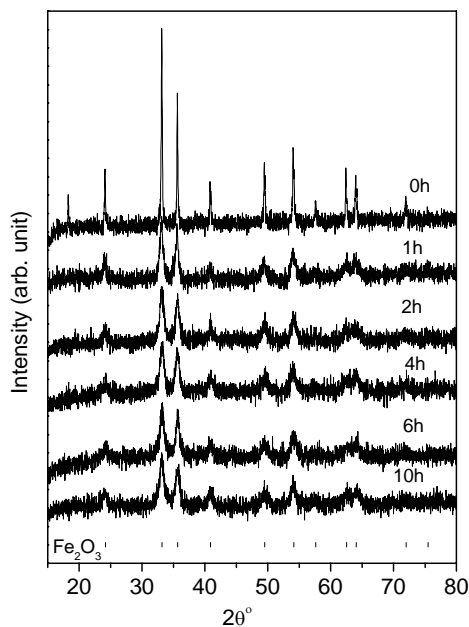

Figure1. X-ray diffraction patterns of α- Fe_2O_3 powder samples in unmilled and milled states

Table 1. Summary of parameters extracted by Rietveld analysis from X-ray diffraction data

Milling time, h	Specimen Name	Phases	Lattice parameters nm		Particle size, nm	RMS strain $<\varepsilon_L^2>^{1/2}$ x 10^3
			a	c		
0	S_0	Hematite	0.5035	1.3753	79.95	0.03
1	S_1	Hematite	0.5036	1.3761	11.03	7.72
2	S_2	Hematite	0.5033	1.3751	10.96	9.17
4	S_4	Hematite	0.5033	1.3745	9.06	8.67
6	S_6	Hematite	0.5030	1.3746	7.63	6.27
10	S_{10}	Hematite	0.5030	1.3776	7.52	6.20

Figure 2 is the TEM micrograph of the specimen milled for 1 hr. This is typical for the other sample. Evidently there are distributions of particle sizes. Figure 3 show distribution of particle sizes in this specimen measured from Fig. 2.The solid lines are the theoretical curves of a log normal distribution function [16] fitted to the experimental data represented by the points in the figures. The former is given by:

$$\Delta n = \frac{1}{\sqrt{2\pi}} \frac{1}{\ln \sigma} \exp\{-\frac{1}{2}[\ln(x/\bar{x})/\ln \sigma]^2\}\Delta(\ln x) \qquad (1)$$

Where Δn is the fractional number of particles per logarithm diameter interval Δ(lnx), $\bar{x}$ is the median diameter, and σ the
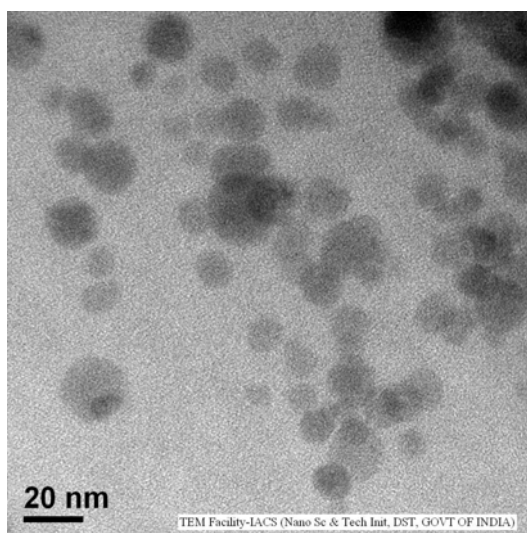

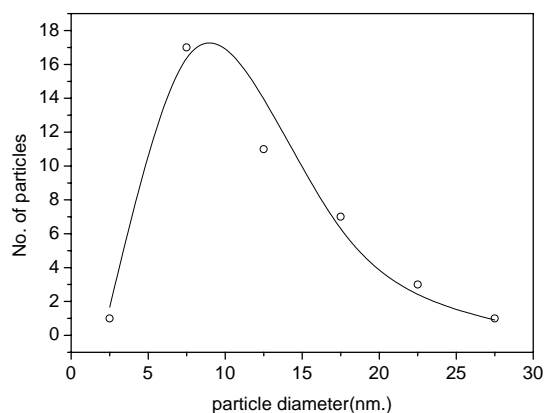Figure 2. TEM micrograph of the specimen milled for 1 h

Figure 3. Distribution of particle size in the specimen milled for 1 h (measured from TEM micrograph in Fig. 2)

Table 2. Extracted Values of Median diameter and geometric standard deviation as determined from TEM Figures

Specimen Name	Median diameter ($\bar{x}$) (nm)	Standard deviation (σ)
S_1	11.9	1.57
S_{10}	8.05	1.57

geometric deviation. The extracted values of median diameter ($\bar{x}$) and geometric standard deviation σ of the specimens milled for 1 h and 10 h are included in Table 2. We identified the hematite phase from the electron diffraction pattern (not shown in the figure). Apart from α-Fe_2O_3 major phase, trace amount of wüstite (FeO) can be identified from the weak electron diffraction rings. It has been reported that α-Fe_2O_3 transformed to Fe_3O_4 and, subsequently to the FeO phase when α-Fe_2O_3 powder was ball milled in air atmosphere [17].

The variation of log resistivity as a function of inverse temperature is represented in Fig. 4 for all the specimens. The resistivity variation of the bulk α- Fe_2O_3 particles can be assigned to typical band conduction. A substantial decrease of resistivity is observed for the specimen milled for various hours.
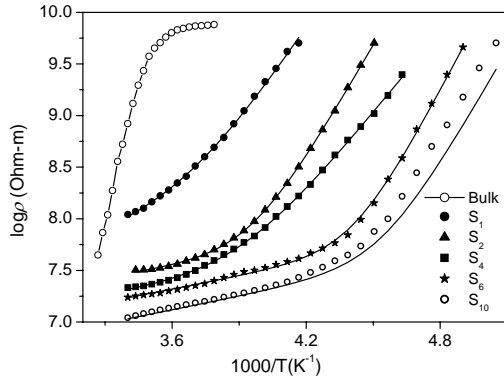

Figure 4. Variation of log resistivity as a function of inverse temperature for all the specimens

It is evident that the resistivity variation of these milled samples is controlled by more than one thermally activated process. The data of the milled specimen have been fitted to equation 2 which incorporates two activated mechanisms

$$\rho = f\rho_1 + (1-f)\rho_2 \qquad (2)$$

Where ρ is the over all resistivity and ρ_1, ρ_2 are the resistivities due to the two activated processes, and f is the volume fraction contributing to the process represented by ρ_1.

We also represent ρ_1 and ρ_2 by the following relations:

$$\rho_1 = \rho_{01} \exp(W_1 / kT) \qquad (3)$$

$$\rho_2 = \rho_{02} \exp(W_2 / kT) \qquad (4)$$

Where ρ_{01} and ρ_{02} are the pre exponential factors, W_1 and W_2 are the two activation energies, k is the Boltzmann constant and T is the temperature. The theoretically fitted curves are shown in Fig. 4 by the solid lines. The agreement between the theoretical fits and experimental data is satisfactory. The parameters obtained by the fitting procedure are summarized in Table 3.

Table 3. Parameters extracted by fitting resistivity data using Eqs. (2) to (4)

Sample Name	ρ_{01} (Ohm-m)	W_1 (eV)	ρ_{02} (Ohm-m)	W_2 (eV)	f
S_1	5.89×10^5	0.16	2.3×10^{-4}	0.64	0.25
S_2	6.94×10^6	0.06	1.12×10^{-7}	0.73	0.32
S_4	5×10^6	0.06	1.6×10^{-4}	0.52	0.35
S_6	9.5×10^5	0.08	7.56×10^{-11}	0.81	0.66
S_{10}	4.66×10^5	0.086	1.11×10^{-9}	0.74	0.74

Observed temperature dependence of resistivity of the as milled α-Fe_2O_3 compacted specimens can be ascribed to a transition from band conduction (i.e. of unmilled α-Fe_2O_3 particles) to surface conduction across the α-Fe_2O_3 nanoparticles. The appearance of two activation mechanisms for the ball-milled specimens suggests a contribution arising from the participation of α-Fe_2O_3 nanoparticles with lower average particle size and other with higher average particle size in the overall conduction process. The predicted model of conduction seems to be justified from our observed wide distribution of particle sizes for the various ball milled oxide particles. Mean particle size varies from 11.5 nm to 8 nm with the progress of milling time. It is evident from Table 3 that upon increasing the duration of milling volume fraction of the nanoparticles with lower mean particle size increases and that of the higher mean particle size decreases. As a result enhancement of low energy (i.e. W_1) activated region and reduction of high energy (i.e. W_2) activated region are observed in the temperature dependence of resistivity.

Conclusions

Electrical resistivity of compacted bulk Hematite (α-Fe_2O_3) powder was found to drop significantly as it was ball milled for few hours. Resistivity data could be characterized by more than one thermally activated process depending upon the duration of milling. Distribution of particle size dominates in thermally activated conduction processes in case of nanostructured Ferric oxide system.

References

1. D. Chakravorty and A.K. Giri, *Chemistry of Advanced Materials*, ed C.N. Rao (Blackwell Scientific publications, Oxford, 1992) p. 217.
2. R.L. Whetten, D.M. Cox, D.J. Trevor and A. Kaldor, *Phys. Rev. Lett.,* 54 (1988) 1494.
3. H.Gleiter, *Prog. Mater. Sci.,* 33 (1989) 223.
4. H.Sankur and J.T.Cheung, *Appl. Phys. A,* 47 (1988) 271
5. M.M. Kapper, Martin Schär, Peter Radi, Ernest Schumacher, *J. Chem. Phys.,* 84 (1986) 1863.
6. R. Biringer, H. Gleiter, H.P. Klein, P. Marquardt, *Phys. Lett. A* , 120 (1984) 365.
7. M. Nogami, K. Nagarka, E. Kato, *J. Amer. Ceramic Soc.*, 73 (1990) 2097.
8. D. Chakravorty, *Bull. Mater. Sci.,* 6 (1984) 193.
9. T. Nakanishi, Bunsho Ohtani, Kohei Uosaki, *Jpn. J.Appl. Phys.,* 36 (1997) 4053.
10. S. Roy and D. Chakravorty, *Appl. Phys. Lett.,* 59 (1991) 4053.
11. C.C. Koch, *Ann. Rev. Mater. Sci.,* 19 (1994) 1032.
12. P.Ayyub, V.R.Palker, M.S.Multani, *Phys.Rev.B,* 51 (1995) 6135.
13. M. Shiojiri, C. Kipo, *J. Cryst. Growth,* 52 (1981) 170.
14. H. Pal, A Chanda, M. De, *J. Alloys Comp.,* 278 (1988) 209.
15. H.M. Rietvelt, *J. Appl. Crystallogr.*, 2 (1969) 65; P. Bose, S. Bid, S.K. Pradhan, M. Pal, D. Chakravorty, *J. Alloys Compd.,* 343 (2002) 192
16. D. Das, S. Roy, J.W. Chen, D. Chakravorty, *J. Appl. Phys.,* 91 (2002) 4573.
17. T. Cosmac, T.H. Courtney, *J. Mater. Res.* 7, (1992) 1519.